Characterizing land surface energy budget under varying climatic conditions from AVIRIS and MASTER data

Shunlin Liang, Dongdong Wang

Tao He, Qinqing Shi

Department of Geographical Sciences

University of Maryland, College Park

2013 HyspIRI Science Workshop

Pasadena, CA. Oct 15-17 2013

UNIVERSITY OF MARYLAND

Objectives

Quantification of the variations in land surface radiation and energy budget over different land cover types in response of climate variability from the AVIRIS and MASTER data to support the development of the HyspIRI mission.

1. Mapping the surface radiation and energy budget components from both AVIRIS and MASTER data.
   - ❑ Algorithm development/refinement
   - ❑ Algorithm and data validation
   - ❑ Mapping of surface radiation and energy budget components
2. Quantifying the variations in surface energy budget of different surface types.
   - ❑ Mapping land cover types from AVIRIS and MASTER data
   - ❑ Assessing variations in those surface radiation and energy budget components of different cover types under various climate conditions
   - ❑ Addressing a set of scientific questions using these datasets

UNIVERSITY OF MARYLAND

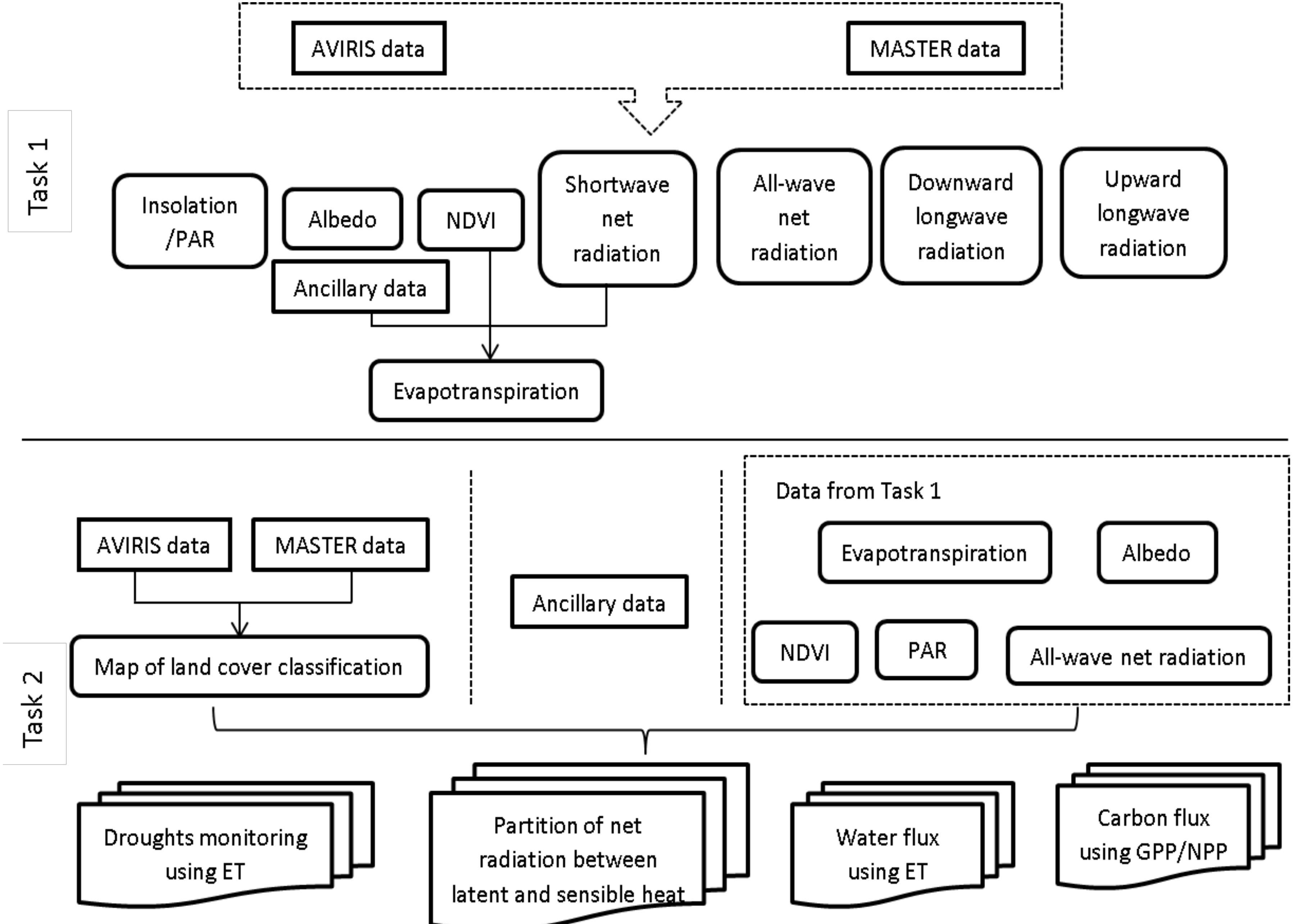

AVIRIS data
MASTER data
Task 1
Insolation /PAR
Albedo
NDVI
Shortwave net radiation
All-wave net radiation
Downward longwave radiation
Upward longwave radiation
Ancillary data
Evapotranspiration
AVIRIS data
MASTER data
Map of land cover classification
Ancillary data
Data from Task 1
Evapotranspiration
Albedo
NDVI
PAR
All-wave net radiation
Task 2
Droughts monitoring using ET
Partition of net radiation between latent and sensible heat
Water flux using ET
Carbon flux using GPP/NPP

$$R_n = R_n^s + R_n^l = (1-\alpha)F_d^s + F_d^l - \sigma\varepsilon T^4$$

Net radiation

albedo

Insolation

Emissivity

Longwave downward radiation

Skin temperature

Radiation budget

Energy budget

$R_n = H + ET + G$

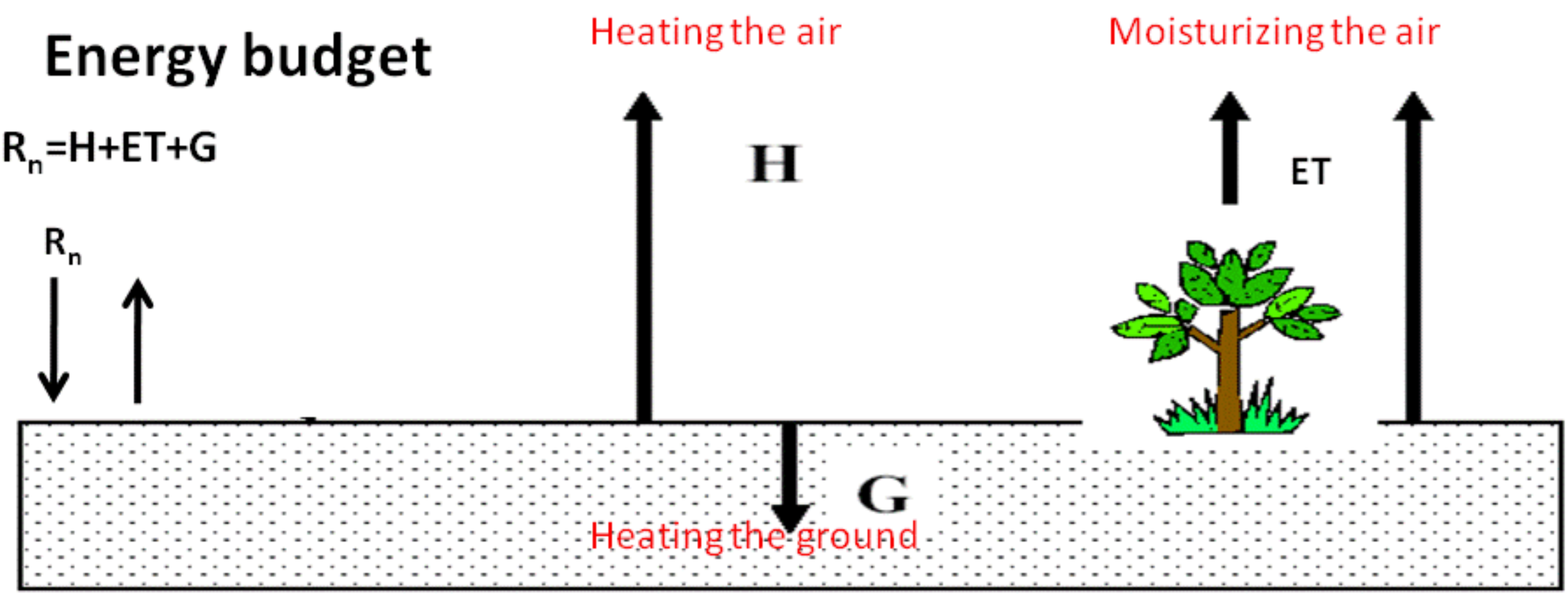

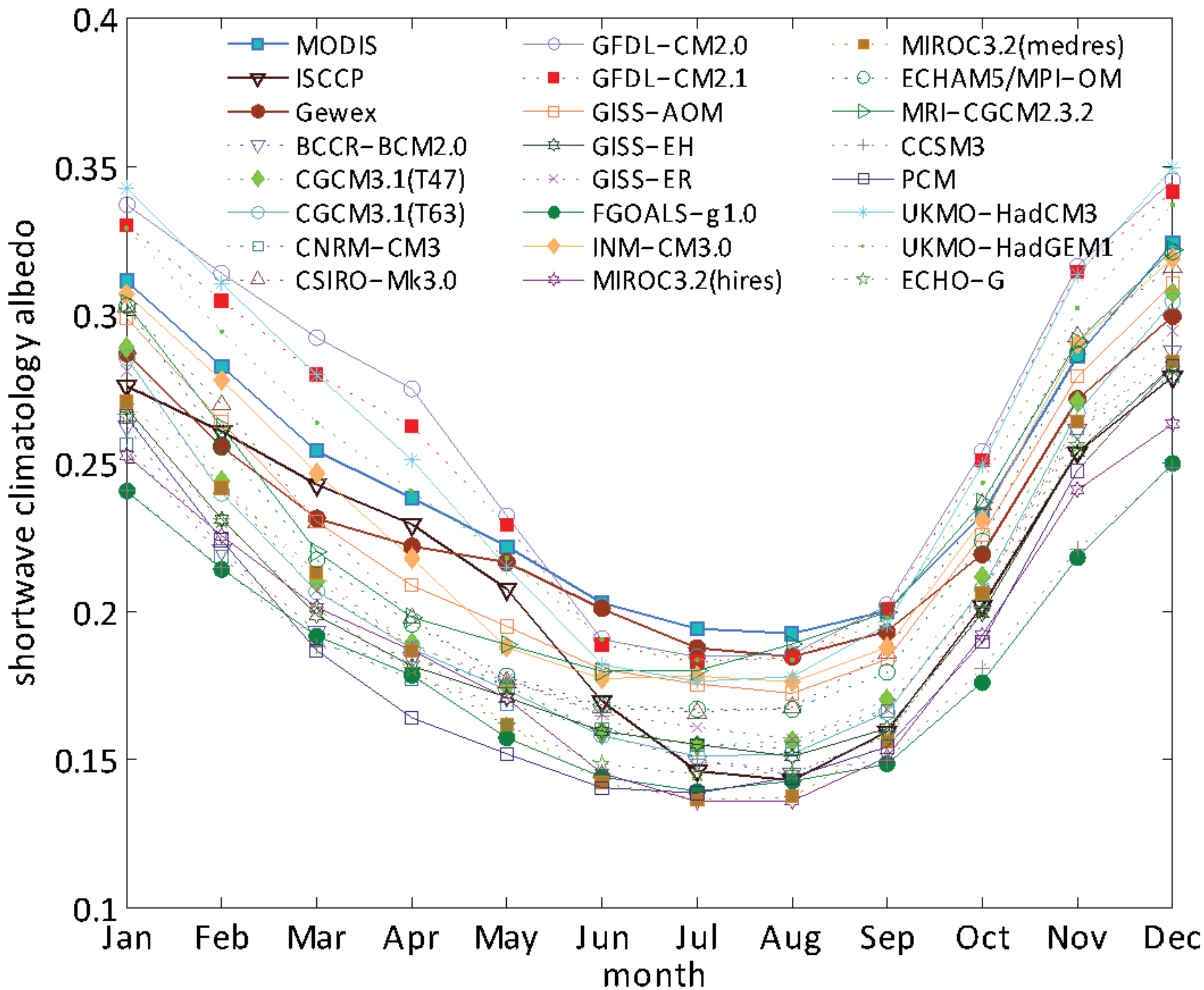

Surface broadband albedo:
IPCC AR4 GCM model simulations
and satellite products

Model mean: 0.21
Standard dev.: 0.02
MODIS: 0.24

MODIS albedo algorithm

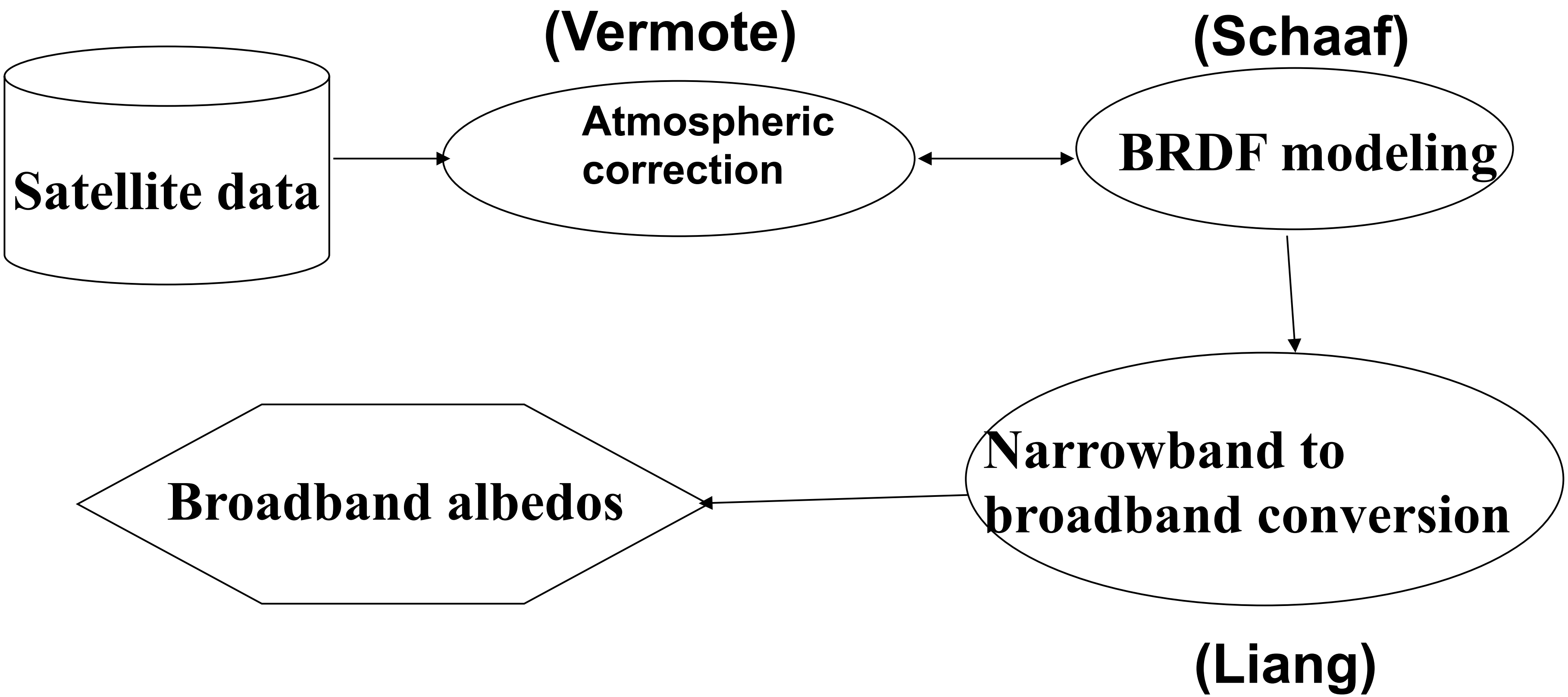

Traditional albedo retrieval algorithms

- Atmospheric correction: based on the “dark-object” method, requiring dense green vegetation canopies;
- Angular modeling: accumulates observations from multiple (16) days but surface conditions may change;
- Narrowband-broadband conversion: based on empirical statistical analysis for average atmospheric conditions with considerable uncertainty;
- Atmospheric correction requires BRDF information & angular modeling requires atmospherically corrected surface reflectance;
- Errors associated with each procedure may cancel or reinforce each other.

UNIVERSITY OF MARYLAND

Direct estimation of surface albedo

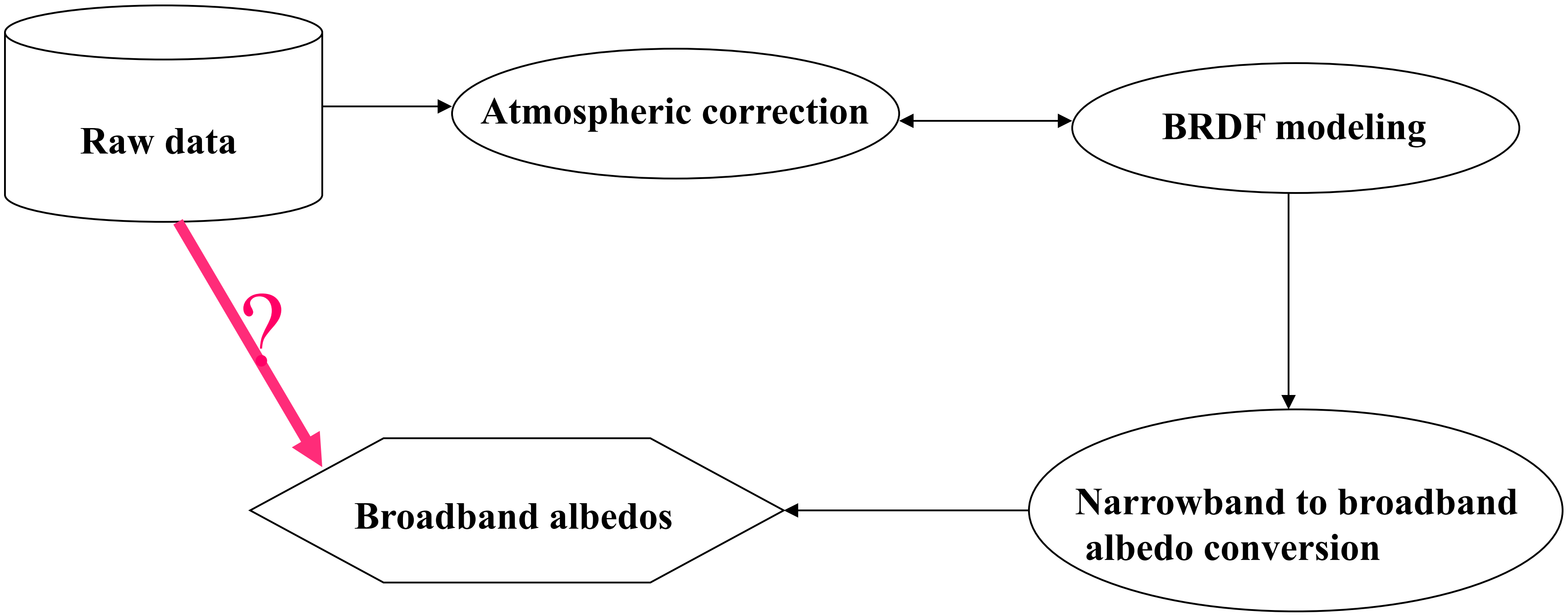

Liang, S., (2003), A direct algorithm for estimating land surface broadband albedos from MODIS imagery, *IEEE Trans. Geosci. Remote Sen.,* 41(1):136-145*;*

Liang, S., J. Stroeve and J. Box, (2005), Mapping daily snow shortwave broadband albedo from MODIS: The improved direct estimation algorithm and validation, *Journal of Geophysical Research.* 110 (D10): Art. No. D10109.

Validation of VIIRS albedo data

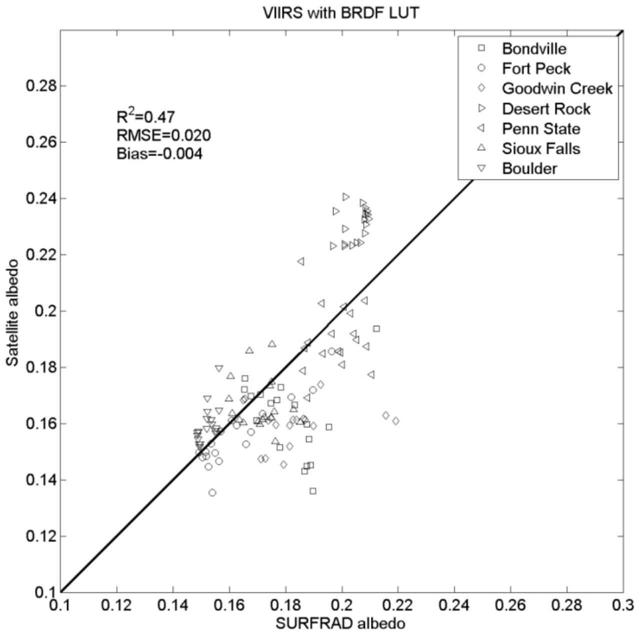

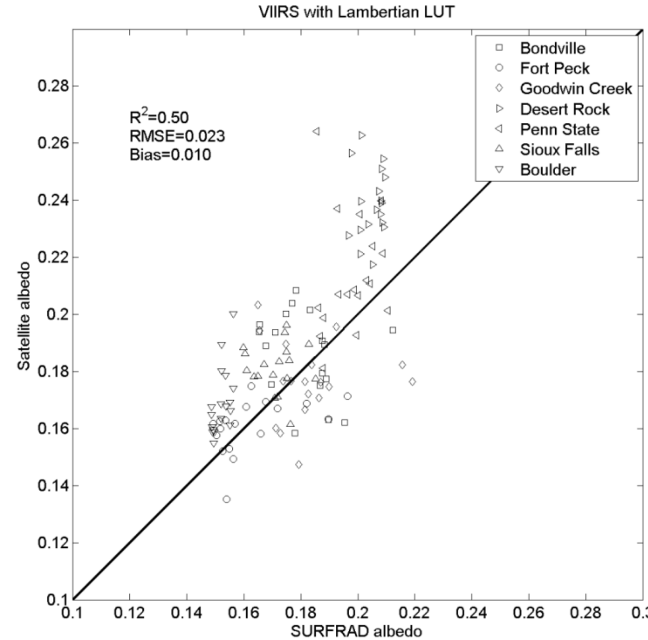

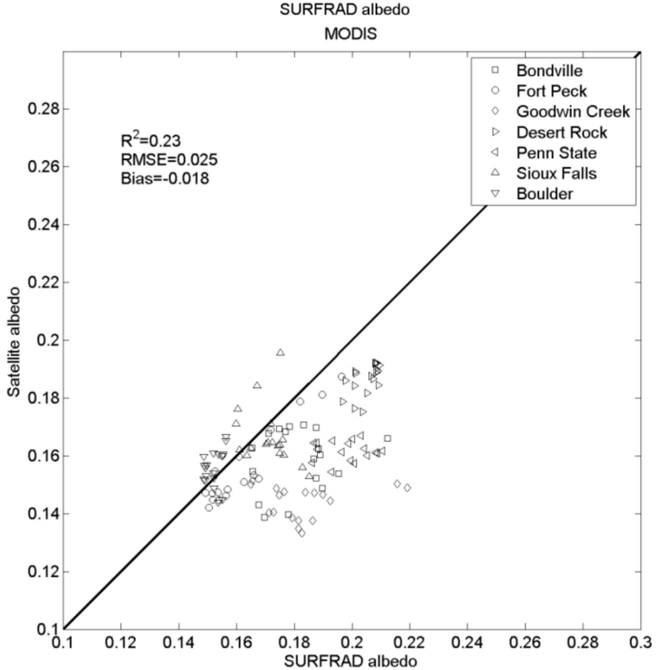

Validation results of 16-day mean albedo from VIIRS BRDF LUT (top left), VIIRS Lambertian LUT (top right) and MODIS (bottom), using data from 2012 non-snow seasons (May-September) at seven SURFRAD sites.

Wang, D., Liang, S., He, T., Yu, Y. 2013. Direct Estimation of Land Surface Albedo from VIIRS Data: Algorithm Improvement and Preliminary Validation. JGR. Revised

Apply and refine to AVIRIS data

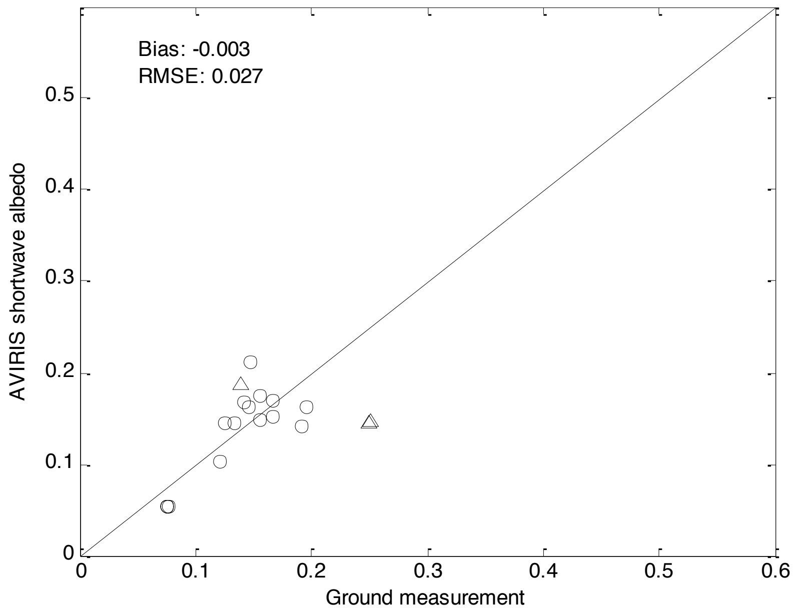

(a)

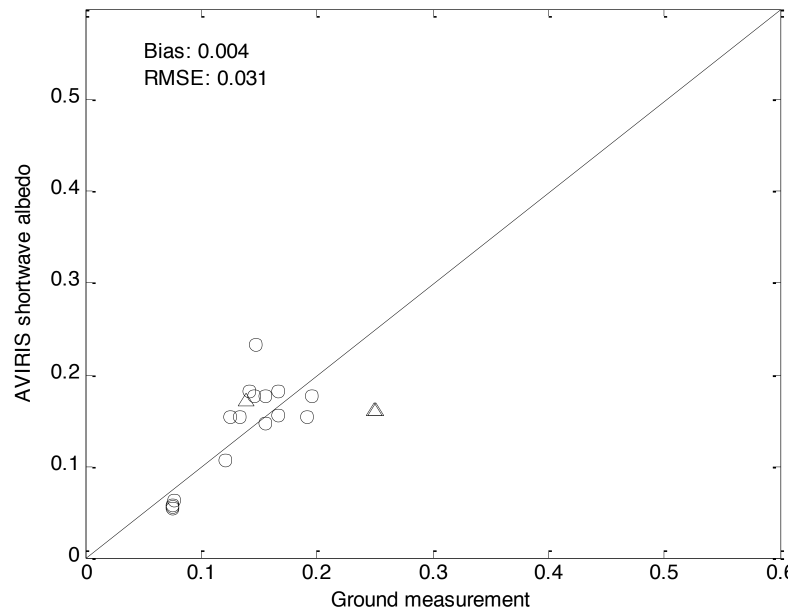

(b)

Comparison of ground measurements AVIRIS shortwave albedo estimates from (a) the stepwise regression algorithm and (b) the PCA-based algorithm at AmeriFlux sites. Statistics shown in the figure are based on flights with resolutions coarser than 8 m (circles). Flights with finer resolutions (<8 m) are denoted in triangles.

He, T., S. Liang, D. Wang, and Q. Shi, (2013). Estimation of high-resolution land surface shortwave albedo from AVIRIS data. *IEEE JSTAR, under review*

UNIVERSITY OF MARYLAND

Mapping surface albedo: AVIRIS vs. Landsat

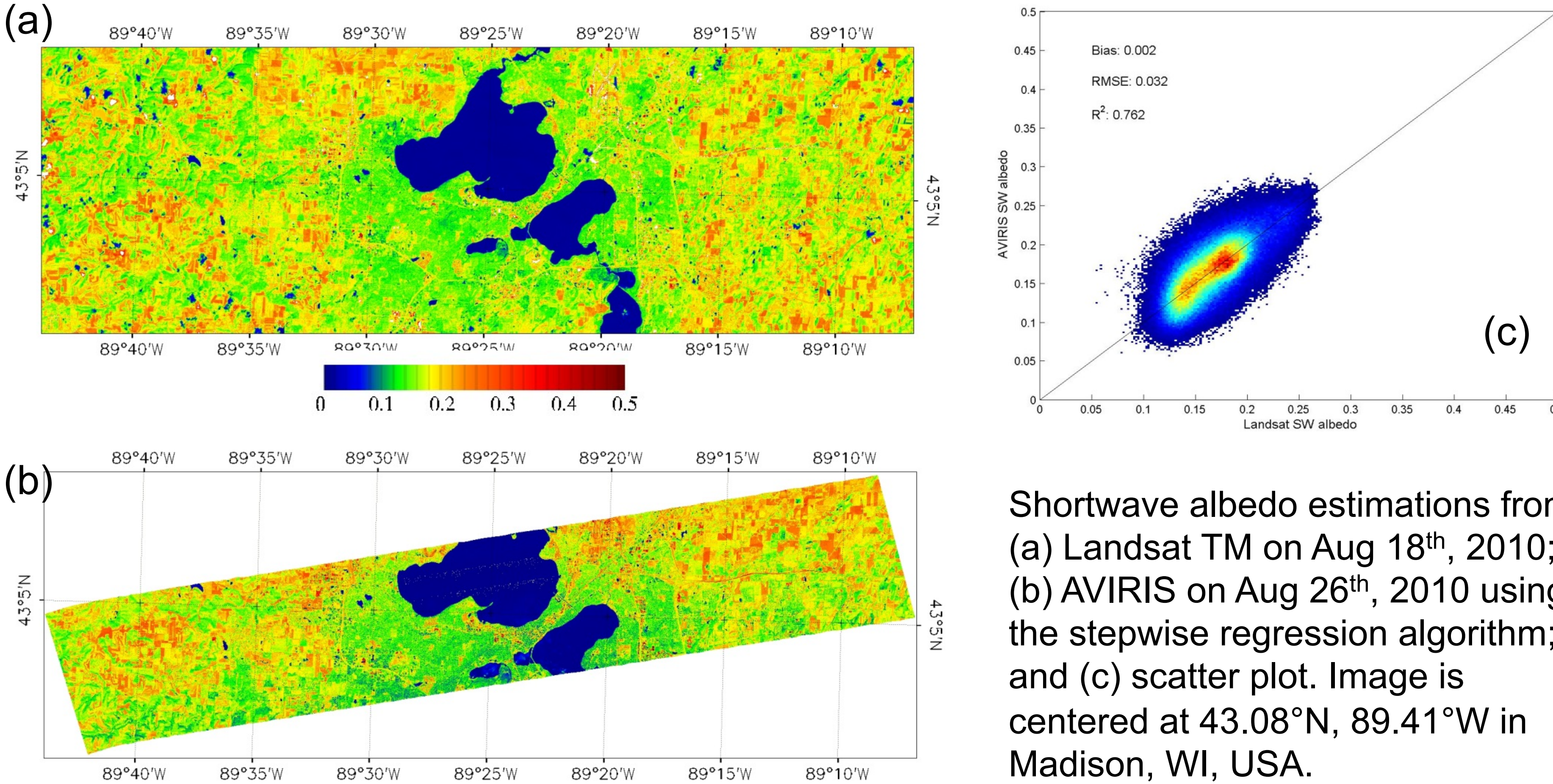

Shortwave albedo estimations from: (a) Landsat TM on Aug 18th, 2010; (b) AVIRIS on Aug 26th, 2010 using the stepwise regression algorithm; and (c) scatter plot. Image is centered at 43.08°N, 89.41°W in Madison, WI, USA.

He et al. 2013

UNIVERSITY OF MARYLAND

Estimation of shortwave net radiation

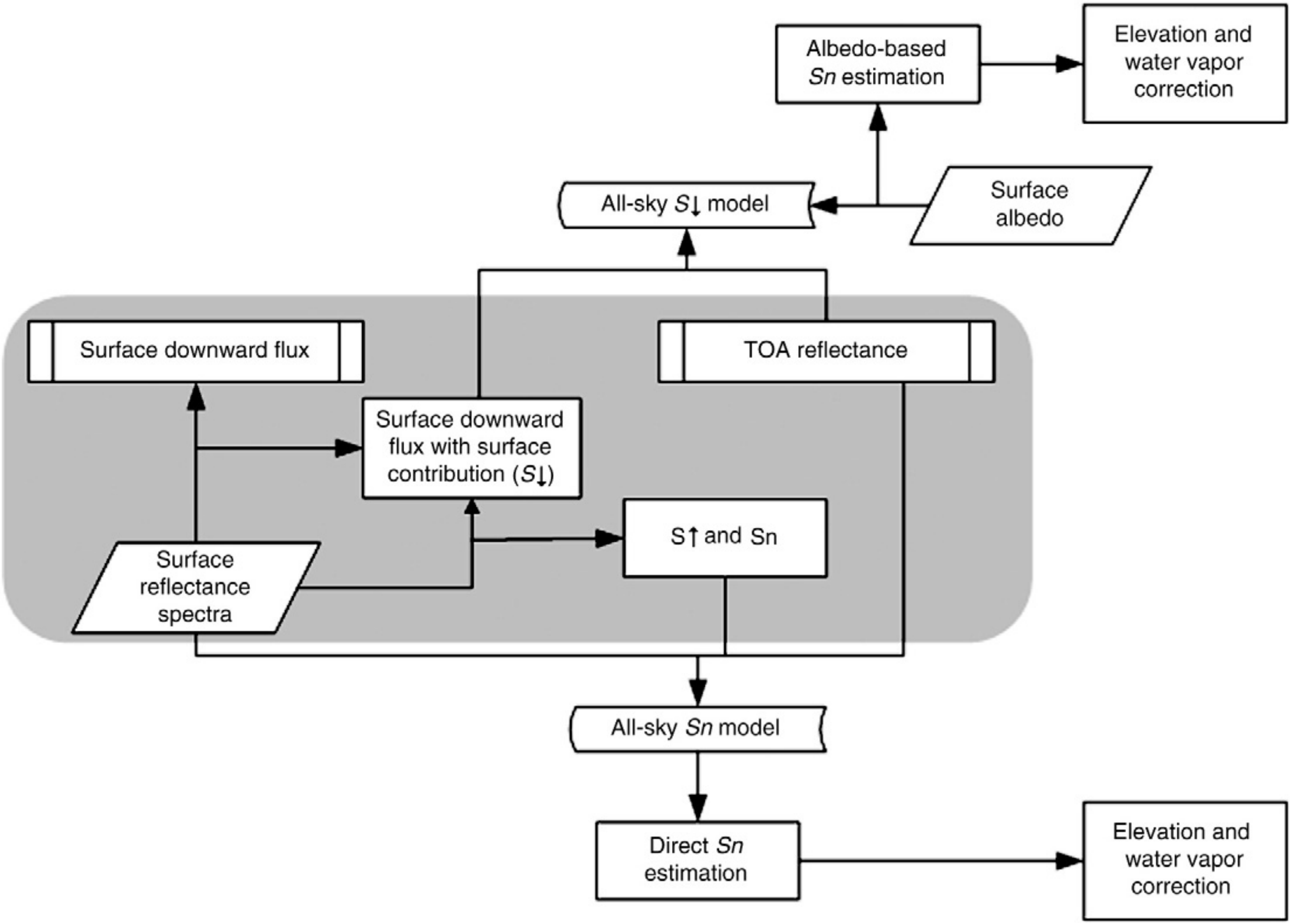

Kim, H.Y., & Liang, S. (2010). Development of a hybrid method for estimating land surface shortwave net radiation from MODIS data. Remote Sensing of Environment, 114, 2393-2402

Algorithm improvement: high resolution Landsat data

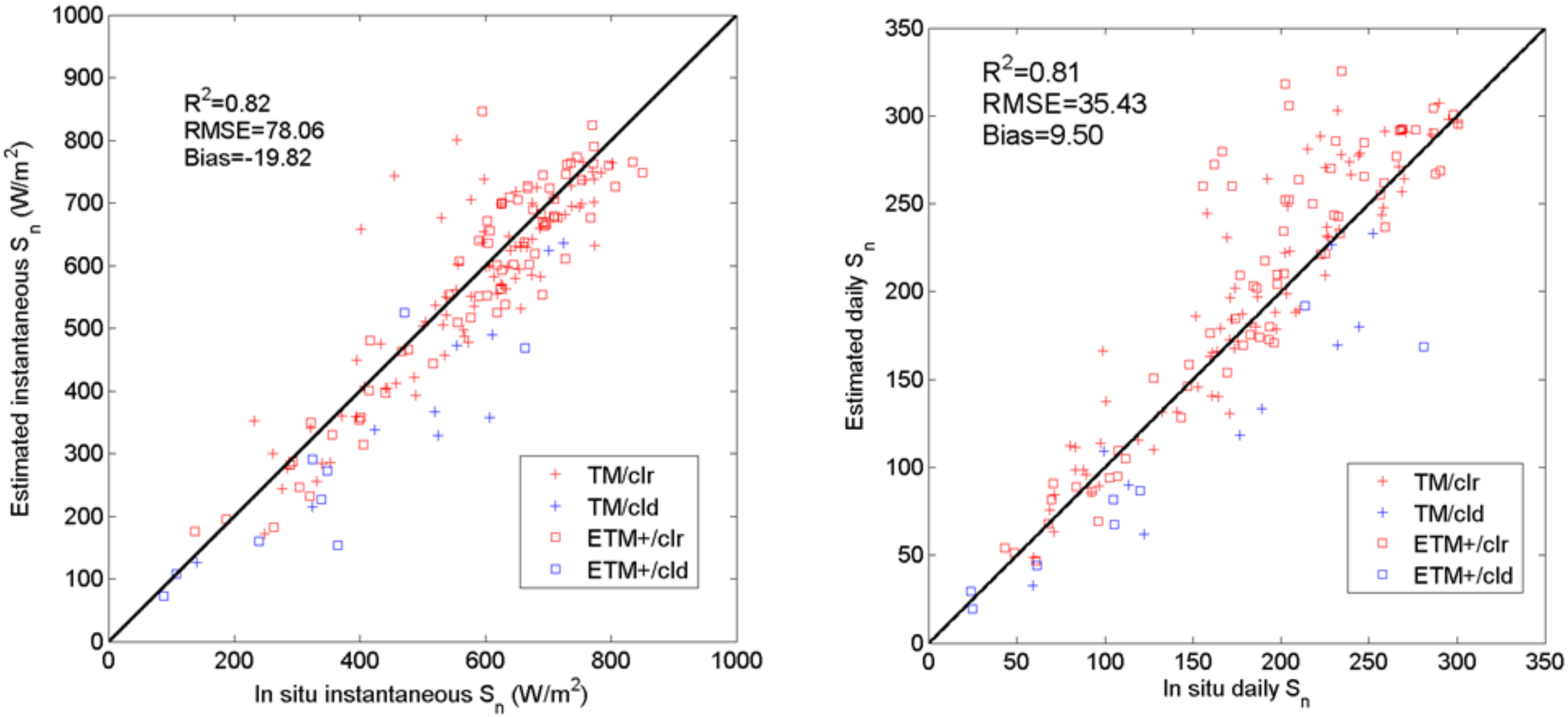

Comparison between instantaneous and daily SSNR (in W/m²) using the method of water vapor correction and in situ measurements at six AmeriFlux sites from 2003-2005.

Wang, D. Liang, S. He, T. 2013. Mapping high-resolution surface shortwave net radiation from Landsat data. IEEE Geoscience and Remote Sensing Letter, in press

UNIVERSITY OF MARYLAND

Estimating shortwave net radiation from AVIRIS

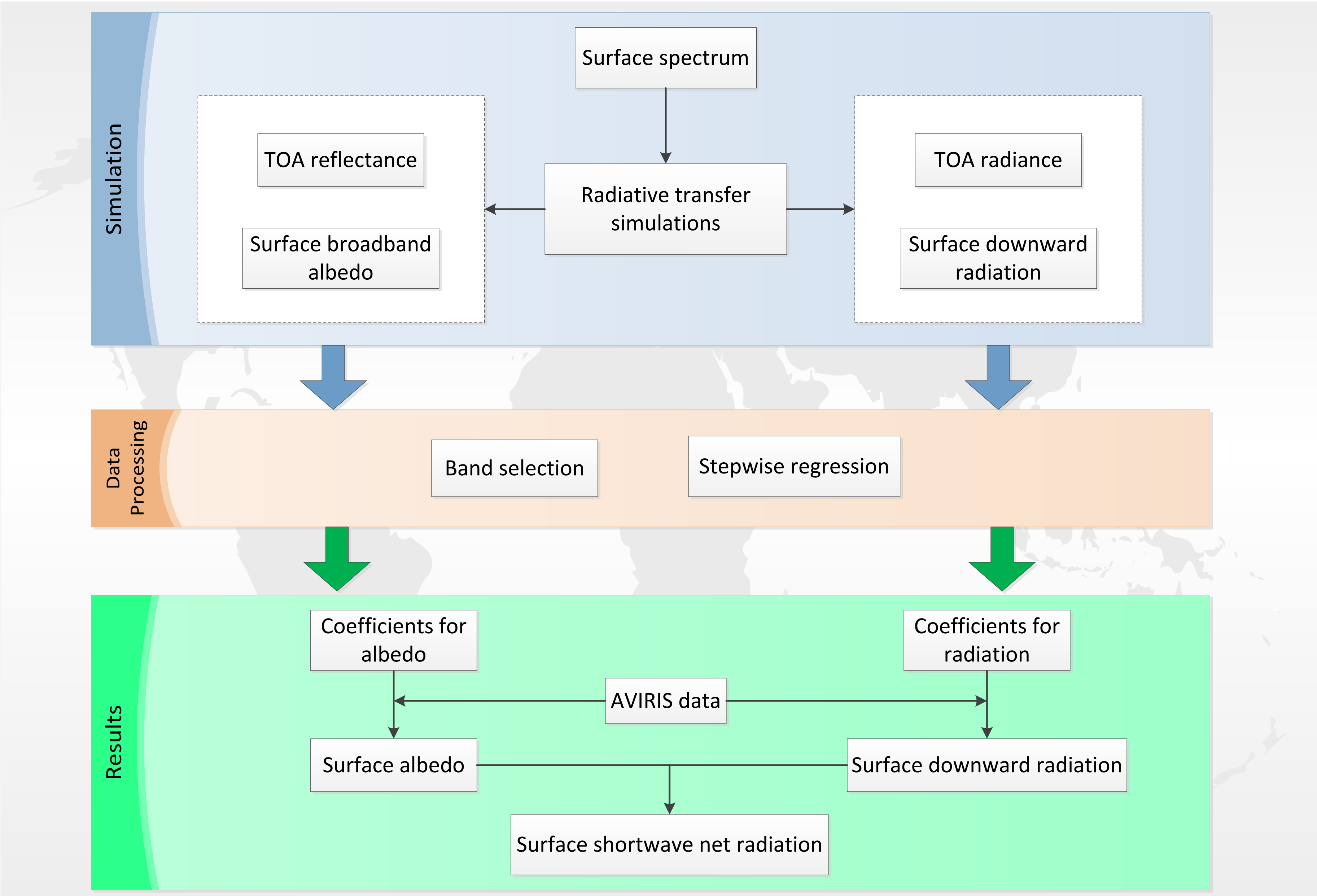

Shortwave radiation estimation: AVIRIS

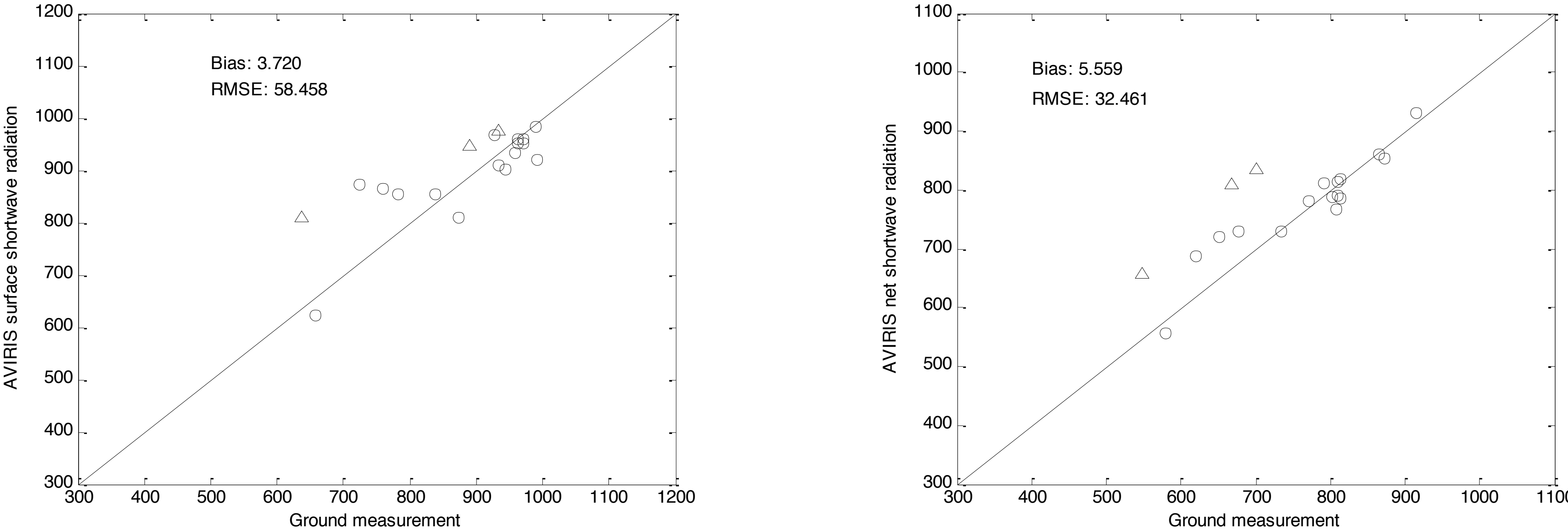

Comparison of ground measurements AVIRIS downward radiation (a) and net radiation (b) estimates at AmeriFlux sites. Statistics shown in the figure are based on flights with resolutions coarser than 8 m (circles). Flights with finer resolutions (<8 m) are denoted in triangles.

He, T., S. Liang, D. Wang, and Q. Shi. Land surface shortwave radiation budget estimation from AVIRIS data. *in preparation*

UNIVERSITY OF MARYLAND

Estimating longwave fluxes

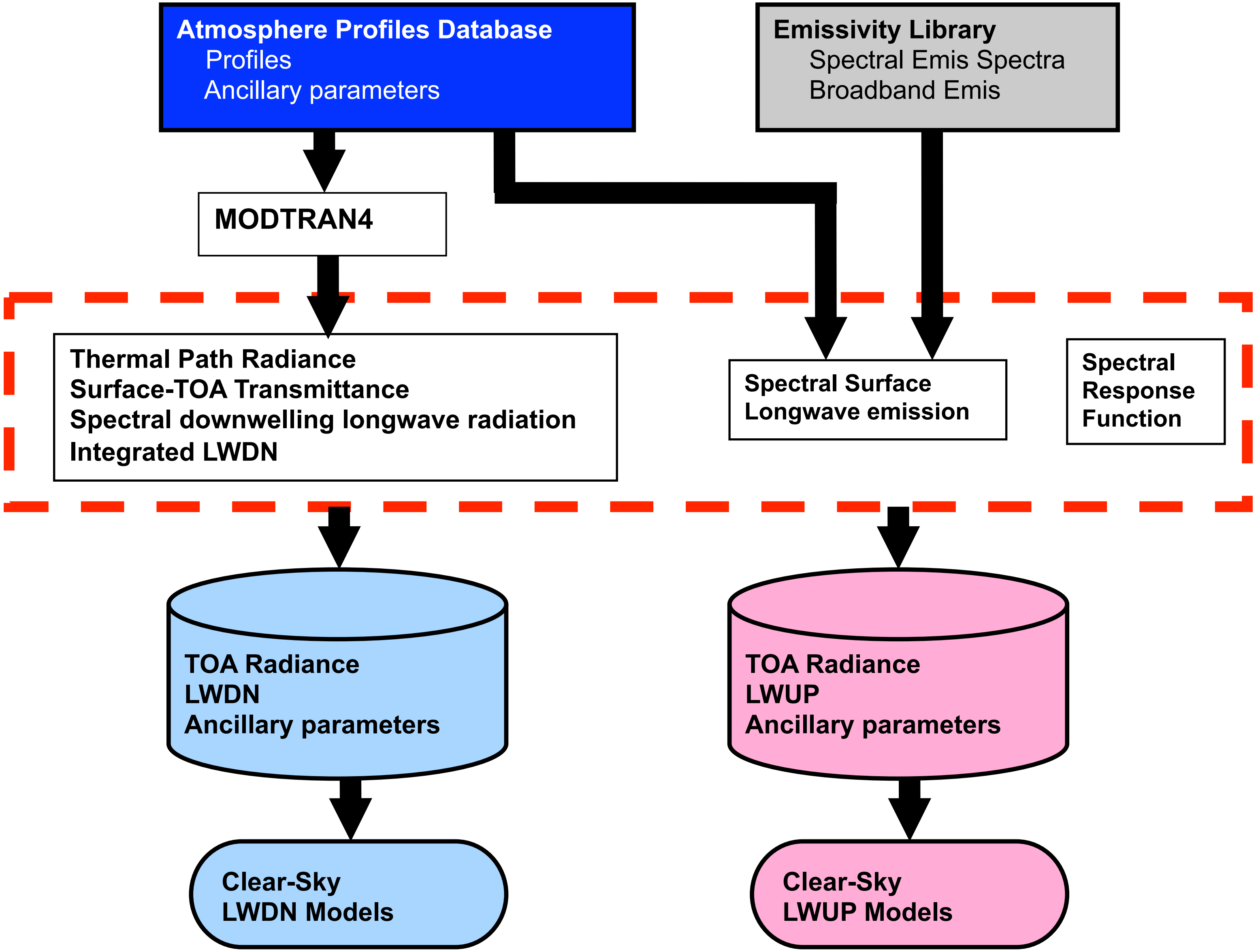

Wang, W., & Liang, S. (2009). Estimating High-Spatial Resolution Clear-Sky Land Surface Downwelling and Net Longwave Radiation from MODIS Data. *Remote Sensing of Environment, 113*, 745-754

Table 5. R^2, Bias, Relative Bias of Satellite Products, STD, and Relative STD of the Differences Between Observed and Satellite-Estimated Clear-Sky LWDN at All Sites for 2003 (Wm^{-2})

	GEWEX-SRB			ISCCP-FD			CERES-FSW			MODIS		
Sites	R^2	Bias(%)	STD(%)	R^2	Bias(%)	STD(%)	R^2	Bias(%)	STD(%)	R^2	Bias(%)	STD(%)
North America												
BON	0.86	−17.7(−5.6)	21.6(6.8)	0.62	−5.2(−1.6)	32.1(10.0)	0.95	3.2(1.1)	15.0(5.0)	0.88	−5.4(−1.8)	22.3(7.4)
TBL	0.79	−23.6(−8.1)	18.4(6.3)	0.58	18.8(6.4)	32.0(10.8)	0.86	−6.4(−2.2)	18.5(6.5)	0.87	1.3(0.5)	18.6(6.5)
DRA	0.94	−29.9(−9.9)	11.4(3.7)	0.76	26.5(8.6)	22.8(7.4)	0.95	−17.7(−5.8)	11.7(3.8)	0.84	−18.2(−5.9)	20.2(6.5)
FPK	0.85	−16.5(−5.7)	20.3(7.0)	0.78	5.6(1.9)	28.2(9.8)	0.92	−3.6(−1.3)	17.9(6.3)	0.93	−4.7(−1.7)	15.7(5.6)
GWN	0.86	−19.9(−5.9)	19.7(5.9)	0.54	−13.0(−3.9)	32.6(9.8)	0.94	−6.3(−2.0)	15.2(4.7)	0.81	−8.2(−2.6)	27.4(8.5)
PSU	0.85	−21.7(−7.1)	21.3(7.0)	0.64	7.2(2.4)	31.7(10.4)	0.92	1.2(0.4)	16.4(5.4)	0.86	−7.3(−2.4)	19.5(6.5)
Mean	0.86	−21.55(−7.1)	18.8(6.1)	0.65	6.7(2.3)	29.9(9.7)	0.92	−4.9(−1.6)	15.8(5.3)	0.87	−7.1(−2.3)	20.6(6.8)
Qinghai-Tibetan Plateau												
Amdo	0.72	−8.8(−5.2)	18.3(10.9)	0.39	34.4(21.9)	24.6(15.6)	0.63	−1.0(−0.6)	21.2(12.3)	0.49	16.0(9.4)	36.2(21.2)
BJ	0.85	−22.6(−10.9)	18.2(8.8)	0.58	39.6(21.5)	25.7(13.9)	0.83	−7.3(−3.7)	18.0(9.1)	0.60	26.3(13.3)	36.4(18.5)
D105	0.72	−7.1(−4.0)	24.6(14.0)	0.49	28.3(17.0)	35.5(21.4)	0.81	−1.9(−1.1)	19.7(11.3)	0.54	17.4(9.9)	34.9(20.0)
Gaize	0.87	−22.2(−11.3)	13.3(6.8)	0.50	21.6(11.0)	37.7(19.3)	0.87	−13.8(−6.8)	15.8(7.8)	0.81	16.4(8.0)	26.4(12.9)
QHB	0.81	−2.5(−1.2)	23.7(10.9)	0.55	4.2(2.1)	39.5(19.4)	0.81	−10.6(−4.7)	23.5(10.6)	0.69	0.0(0.0)	32.1(14.5)
Mean	0.79	−12.6(−6.5)	19.6(10.3)	0.50	25.6(14.7)	32.6(17.9)	0.79	−6.9(−3.4)	19.6(10.2)	0.63	15.2(8.1)	33.2(17.4)
Southeast Asia												
MKL	0.65	−19.1(−4.9)	16.5(4.3)	0.39	−3.5(−0.9)	21.8(5.7)	0.10	−19.7(−5.0)	29.5(7.4)	0.66	−25.4(−6.4)	17.3(4.4)
SKR	0.54	−14.3(−3.7)	13.8(3.5)	0.42	−6.1(−1.6)	17.1(4.4)	0.71	−13.1(−3.4)	10.5(2.7)	0.55	−16.5(−4.3)	12.7(3.3)
Mean	0.60	−16.7(−4.3)	15.2(3.9)	0.41	−4.8(−1.3)	19.5(5.1)	0.41	−16.4(−4.2)	20.0(5.1)	0.61	−21.0(−5.4)	15.0(3.9)
Japan												
TKY	0.59	−41.5(−12.9)	34.1(10.6)	0.56	−14.5(−4.4)	36.9(11.3)	0.66	−16.7(−5.4)	22.6(7.2)	0.82	−29.8(−9.5)	16.1(5.2)
TMK	0.73	−19.8(−6.4)	23.4(7.6)	0.66	−5.0(−1.7)	27.7(9.4)	0.77	−12.2(−4.0)	19.8(6.6)	0.87	−17.7(−5.9)	14.5(4.8)
Mean	0.66	−30.7(−9.7)	28.8(9.1)	0.61	−9.8(−3.1)	32.3(10.4)	0.72	−14.5(−4.7)	21.2(6.9)	0.85	−23.8(−7.7)	15.3(5.0)
Four Regions Combined												
All Mean	0.73	−20.4(−6.9)	20.6(7.4)	0.54	4.4(3.2)	28.6(10.8)	0.71	−10.7(−3.5)	19.2(6.9)	0.74	−9.2(−1.8)	21.0(8.3)

Gui, S., Liang, S.L., & Li, L. (2010). Evaluation of satellite-estimated surface longwave radiation using ground-based observations. *Journal of Geophysical Research-Atmospheres, 115*

LW estimation from MASTER data

- MODTRAN5 is used to simulate longwave radiative transfer of MASTER data
  – Database of atmospheric profile (SeeBor V5.0) is used.
  – A database including various surface types is used as the inputs of emissivity.
  – Variations of view zenith angle are considered.

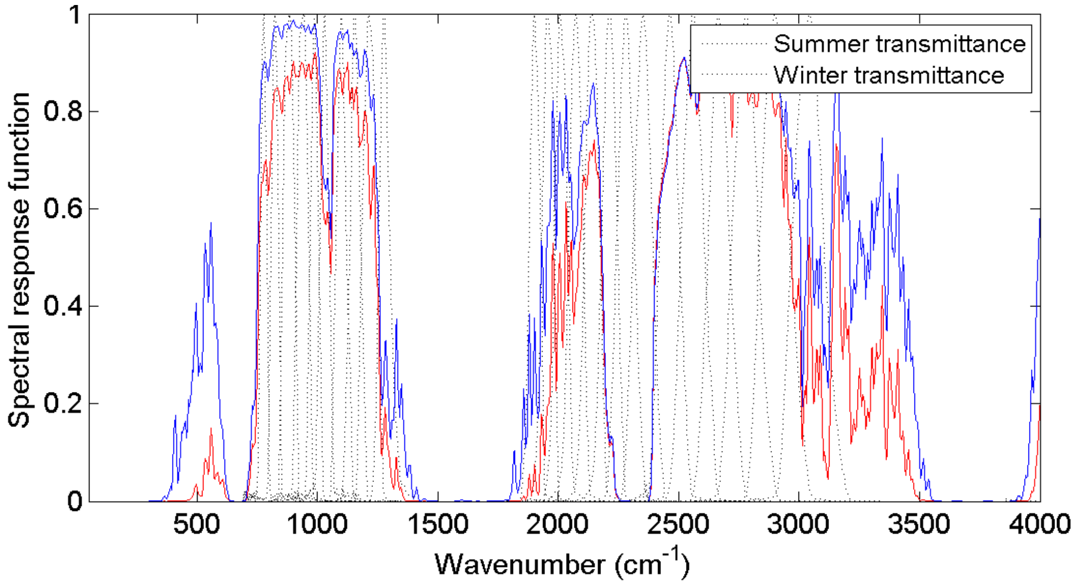

- MASTER has 50 bands, 25 of them are visible and NIR.
- 10 of them are thermal infrared bands.
- Some bands (41,49,50) have many pixels filled

UNIVERSITY OF MARYLAND

Mapping ET

- We will start with the improved regression model that maps global ET using the satellite data and ancillary information (Wang and Liang 2008; Wang et al., 2010a,b).
- We will continue to evaluate other ET algorithms
- We plan to map ET by fusing multiple ET products

UNIVERSITY OF MARYLAND

- Wang, K. and Liang, S. (2008), An improved method to estimate evapotranspiration from a combination of net radiation, vegetation index and temperature: Influence of soil moisture. *Journal of Hydrometeorology 9, 712-727*
- Yiao, Y. S. Liang, Q. Qin, and K. Wang, (2010), Monitoring Drought over the Conterminous United States from MODIS and NCEP Reanalysis-2 Data, *Journal of Applied Meteorology and Climatology*, 49(8), 1665-1680
- Yiao, Y. S. Liang, Q. Qin, and K. Wang, S. Zhao, (2010), Monitoring Global Land Surface Drought Based on an Improved Evapotranspiration Model, *International Journal of Applied Earth Observation and Geoinformation,* 12(6): S266-S776
- Wang, K., B. Dickinson, M. Wild, S. Liang, (2010),Evidence for Decadal Variation in Global Terrestrial Evapotranspiration between 1982 and 2002, Part 1: Model Development", *Journal of Geophysical Research - Atmospheres* , 115, D20112
- Wang, K., B. Dickinson, M. Wild, S. Liang, (2010),Evidence for Decadal Variation in Global Terrestrial Evapotranspiration between 1982 and 2002, Part 2: Results", *Journal of Geophysical Research – Atmospheres* , 115, D20113
- Xu, T., S. Liu, S. Liang, & J. Qin, (2011), Improving Predictions of Water and Heat Fluxes by Assimilating MODIS Land Surface Temperature Products into Common Land Model, *Journal of Hydrometeorology* , 12:227-244
- Xu, T., S. Liang, S. Liu, (2011), Estimating turbulent fluxes through assimilation of geostationary operational environmental satellites data using ensemble Kalman filter, *Journal of Geophysical Research*, 116, D09109, doi:10.1029/2010JD015150
- Yiao, Y. S. Liang, Q. Qin, and K. Wang, S. Zhao, (2011), Monitoring Global Land Surface Drought Based on a hybrid Evapotranspiration Model, International Journal of Applied Earth Observation and Geoinformation, 13(3): 447-457
- Yao, Y., S. Liang, Q. Qin, K. Wang, S. Liu, S. Zhao, N. Zhang, H. Dong, (2012), Satellite detection of the increases in global land surface evapotranspiration during 1984-2007, International Journal of Digital Earth, 5, 299-318
- Li, X., S. Liang, G. Yu, W. Yuan, et al. Estimation of Evapotranspiration over the Terrestrial Ecosystems in China. *Ecohydrology*

Field campaign

- We participated the field campaign in CA this August.
- Land cover, surface spectra, AOD, and LAI data were collected.
- Our capability to measure surface radiation and energy balance components is limited. Measurements of such variables need to exactly match with flights, due to their temporal dynamics.

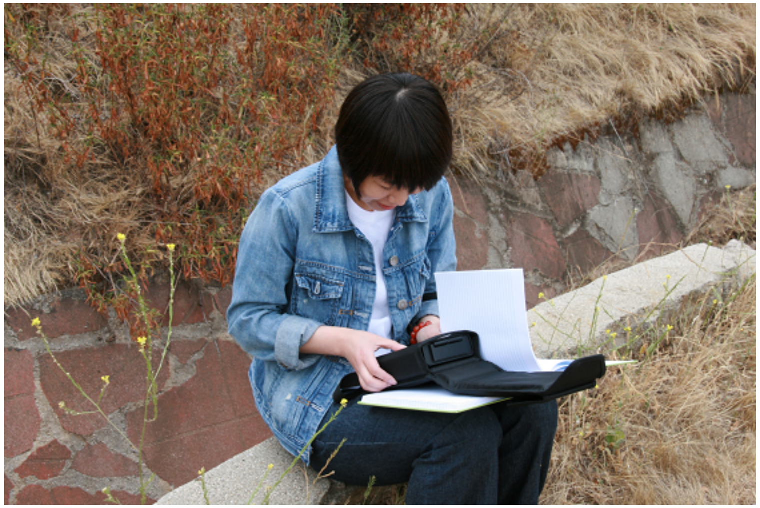

UNIVERSITY OF MARYLAND

Other tasks

- Mapping land cover types from AVIRIS data
- Mapping gross primary productivity (GPP) using the Eddy covariance production efficiency model - EC-PEM (Yuan et al., 2007,2010)
- Evaluation of changes of surface radiation and energy budgets and GPP under different climate and land cover conditions

UNIVERSITY OF MARYLAND

Preliminary Result of Land Cover Mapping

AVIRIS Bands 10-60 surface reflectance, F130522t01p00r11

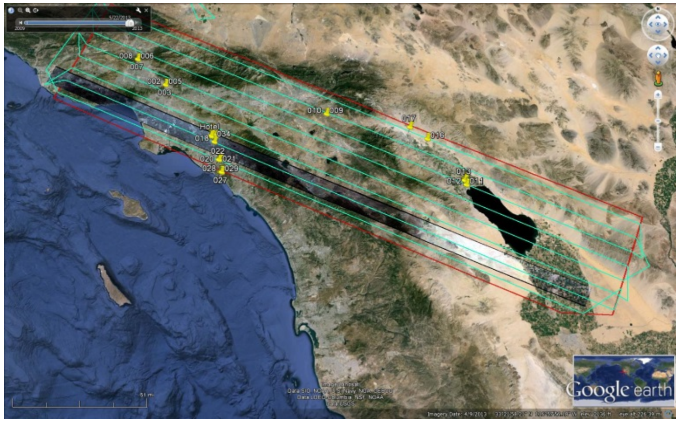

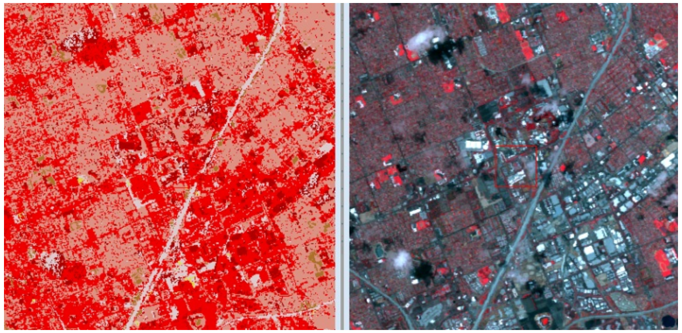

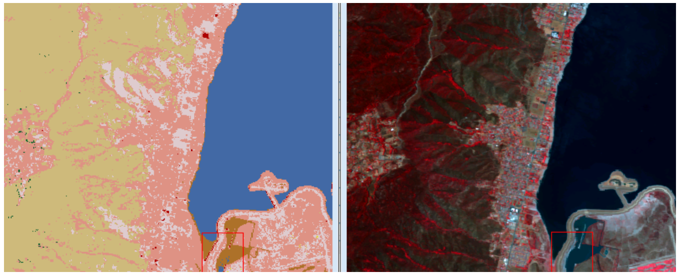

RGB: Band 53,30,20
(850 nm, 650 nm, 550 nm)

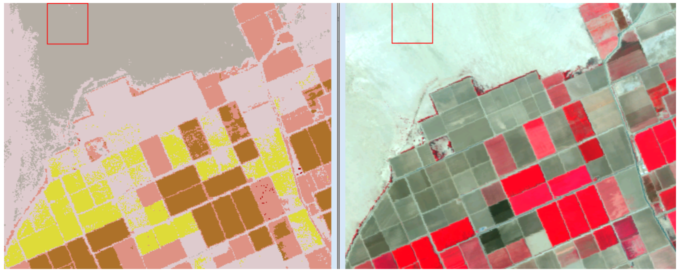

NLCD Land Cover Classification Legend

11	Open Water
12	Perennial Ice/ Snow
21	Developed, Open Space
22	Developed, Low Intensity
23	Developed, Medium Intensity
24	Developed, High Intensity
31	Barren Land (Rock/Sand/Clay)
41	Deciduous Forest
42	Evergreen Forest
43	Mixed Forest
51	Dwarf Scrub*
52	Shrub/Scrub
71	Grassland/Herbaceous
72	Sedge/Herbaceous*
73	Lichens*
74	Moss*
81	Pasture/Hay
82	Cultivated Crops
90	Woody Wetlands
95	Emergent Herbaceous Wetlands

* Alaska only

UNIVERSITY OF MARYLAND

Four Observation Networks of Surface Energy Budget over US

- **SURFRAD**, 7 sites, surface radiation budget
  - The continental U.S. comprising the Surface Radiation Network
  - http://www.esrl.noaa.gov/gmd/grad/surfrad/sitepage.html
- **AmeriFlux**, level 2, 107 sites in USA, surface energy budget
  - Regional network of FLUXNET
  - http://public.ornl.gov/ameriflux/
- **ISIS**, 9 site, insolation
  - NOAA Integrated Surface Irradiance Study (ISIS)
  - http://www.esrl.noaa.gov/gmd/grad/isis/isissites.html
- **BSRN**, 11 sites in USA, surface radiation budget
  - Baseline Surface Radiation Network
  - Including 7 site of Surfrad and 4 other sites
  - http://www.bsrn.awi.de/en/home/bsrn/

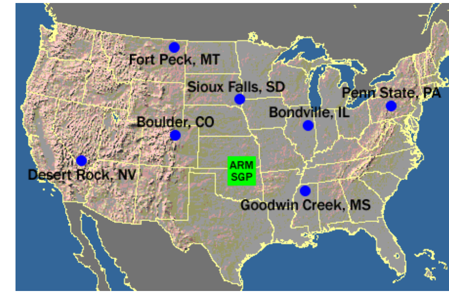

Surfrad

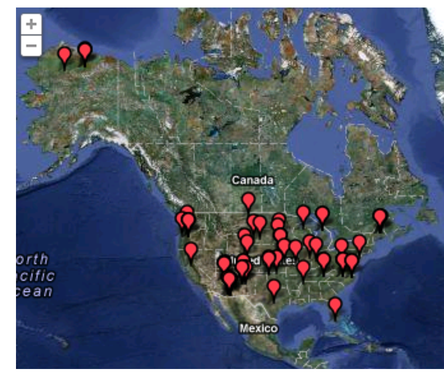

Ameriflux

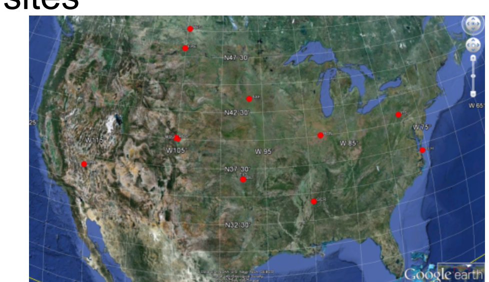

BSRN

ISIS

Overlapped sites and flights

- Temporal period: 2003, 2006-2011, 2013
- Sites from: Surfrad, AmeriFlux, and ISIS
- Method
  - Overlapped temporal coverage
  - Site point location within the boundary of flights
    - Boundary of flights were inferred from the longitude and latitude of four corners

- AVIRIS:
  - 81 scenes from 2241 records
  - AVIRIS summary from archive (2006-2011)

- MASTER:
  - 8 flights from 430 records
  - MASTER summary from all available archives

- Selected flights and sites will be used for validation

MASTER

ID	Site name	Lon	Lat	Flight number	Year	Month	Day
1	US-NR1	-105.55	40.0329	11-667-00	2011	8	7
2	US-Mpj	-106.24	34.4384	10-937-00	2010	7	31
3	US-Seg	-106.7	34.3623	08-001-03	2007	10	4
4	US-Seg	-106.7	34.3623	09-001-02	2008	10	22
5	US-Seg	-106.7	34.3623	11-002-05	2010	10	12
6	US-Ses	-106.74	34.3349	09-001-02	2008	10	22
7	US-Ses	-106.74	34.3349	11-002-05	2010	10	12
8	ISIS_msn	-89.33	43.13	11-669-00	2011	8	10

AVIRIS

ID	Site name	Lon	Lat	Flight number	Year	Month	Day
1	Surfrad_BND	-88.37	40.05	f060802t01p00r07	2006	8	2
2	Surfrad_BND	-88.37	40.05	f060802t01p00r08	2006	8	2
3	Surfrad_TBL	-105.24	40.13	f110807t01p00r16	2011	8	7
4	Surfrad_TBL	-105.24	40.13	f110807t01p00r17	2011	8	7
5	Surfrad_TBL	-105.24	40.13	f110807t01p00r23	2011	8	7
6	Surfrad_PSU	-77.93	40.72	f090706t01p00r06	2009	7	6
7	Surfrad_PSU	-77.93	40.72	f090706t01p00r06	2009	7	6
8	US-Blo	-120.63	38.8952	f070805t01p00r08	2007	8	5
9	US-Ton	-120.97	38.4316	f060512t01p00r02	2006	5	12
10	US-Ton	-120.97	38.4316	f070805t01p00r05	2007	8	5
11	US-Ton	-120.97	38.4316	f070805t01p00r06	2007	8	5
12	US-Ton	-120.97	38.4316	f070805t01p00r07	2007	8	5
13	US-Var	-120.95	38.4067	f060512t01p00r02	2006	5	12
14	US-Var	-120.95	38.4067	f070805t01p00r05	2007	8	5
15	US-Var	-120.95	38.4067	f070805t01p00r06	2007	8	5
16	US-Var	-120.95	38.4067	f070805t01p00r07	2007	8	5
17	US-NR1	-105.55	40.0329	f100825t01p00r07	2010	8	25
18	US-NR1	-105.55	40.0329	f110623t01p00r09	2011	6	23
19	US-NR1	-105.55	40.0329	f110807t01p00r06	2011	8	7
20	US-NR1	-105.55	40.0329	f110807t01p00r10	2011	8	7
21	US-NR1	-105.55	40.0329	f110807t01p00r11	2011	8	7
22	US-NR1	-105.55	40.0329	f110807t01p00r18	2011	8	7
23	US-Skr	-81.078	25.3646	f100523t01p00r12	2010	5	23
24	US-SP3	-82.163	29.7547	f100906t01p00r04	2010	9	6
25	US-SP3	-82.163	29.7547	f100906t01p00r06	2010	9	6
26	US-Bo2	-88.292	40.0061	f060802t01p00r07	2006	8	2
27	US-Bo2	-88.292	40.0061	f060802t01p00r08	2006	8	2
28	US-Bo2	-88.292	40.0061	f060804t01p00r06	2006	8	4
29	US-Bo2	-88.292	40.0061	f060804t01p00r08	2006	8	4
30	US-Ha1	-72.172	42.5378	f090705t01p00r07	2009	7	5
31	US-Ha1	-72.172	42.5378	f090705t01p00r08	2009	7	5
32	US-Ha1	-72.172	42.5378	f090710t01p00r12	2009	7	10
33	US-Ha1	-72.172	42.5378	f090705t01p00r07	2009	7	5
34	US-Ha1	-72.172	42.5378	f090705t01p00r08	2009	7	5
35	US-Ha1	-72.172	42.5378	f090710t01p00r12	2009	7	10
36	US-Ho3	-68.725	45.2072	f090710t01p00r10	2009	7	10
37	US-Ho3	-68.725	45.2072	f090710t01p00r10	2009	7	10
38	US-Ho1	-68.74	45.2041	f090710t01p00r10	2009	7	10
39	US-Ho1	-68.74	45.2041	f090710t01p00r10	2009	7	10
40	US-Ho2	-68.747	45.2091	f090710t01p00r10	2009	7	10
41	US-Ho2	-68.747	45.2091	f090710t01p00r10	2009	7	10
42	US-UMB	-84.714	45.5598	f090704t01p00r10	2009	7	4
43	US-UMB	-84.714	45.5598	f090704t01p00r10	2009	7	4
44	US-UMB	-84.714	45.5598	f110814t01p00r12	2011	8	14
45	US-UMB	-84.714	45.5598	f110816t01p00r13	2011	8	16
46	US-Ne1	-96.477	41.165	f080713t01p00r09	2008	7	13
47	US-Ne1	-96.477	41.165	f080713t01p00r10	2008	7	13
48	US-Ne2	-96.47	41.1649	f080713t01p00r09	2008	7	13
49	US-Ne2	-96.47	41.1649	f080713t01p00r10	2008	7	13
50	US-Ne3	-96.44	41.1797	f080713t01p00r09	2008	7	13
51	US-Ne3	-96.44	41.1797	f080713t01p00r10	2008	7	13
52	US-Bar	-71.288	44.0646	f090710t01p00r09	2009	7	10
53	US-Bar	-71.288	44.0646	f090710t01p00r09	2009	7	10
54	US-ChR	-84.332	35.9311	f090724t01p00r06	2009	7	24
55	US-ChR	-84.332	35.9311	f090724t01p00r06	2009	7	24
56	US-Los	-89.979	46.0827	f080709t01p00r10	2008	7	9
57	US-Los	-89.979	46.0827	f080714t01p00r06	2008	7	14
58	US-Los	-89.979	46.0827	f090729t01p00r07	2009	7	29
59	US-Los	-89.979	46.0827	f090729t01p00r07	2009	7	29
60	US-PFa	-90.272	45.9459	f080709t01p00r10	2008	7	9
61	US-PFa	-90.272	45.9459	f080714t01p00r06	2008	7	14
62	US-PFa	-90.272	45.9459	f090729t01p00r07	2009	7	29
63	US-PFa	-90.272	45.9459	f090729t01p00r07	2009	7	29
64	US-PFa	-90.272	45.9459	f100826t01p00r13	2010	8	26
65	US-CaV	-79.421	39.0633	f090706t01p00r12	2009	7	6
66	US-CaV	-79.421	39.0633	f090706t01p00r12	2009	7	6
67	US-UMd	-84.698	45.5625	f090704t01p00r10	2009	7	4
68	US-UMd	-84.698	45.5625	f090704t01p00r10	2009	7	4
69	US-UMd	-84.698	45.5625	f110814t01p00r12	2011	8	14
70	US-UMd	-84.698	45.5625	f110816t01p00r13	2011	8	16
71	ISIS_hnx	-119.63	36.31	f060919t01p00r09	2006	9	19
72	ISIS_msn	-89.33	43.13	f100826t01p00r07	2010	8	26
73	ISIS_msn	-89.33	43.13	f110730t01p00r17	2011	7	30
74	ISIS_msn	-89.33	43.13	f110810t01p00r07	2011	8	10
75	ISIS_msn	-89.33	43.13	f110814t01p00r16	2011	8	14
76	ISIS_msn	-89.33	43.13	f110816t01p00r08	2011	8	16
77	ISIS_msn	-89.33	43.13	f110816t01p00r09	2011	8	16
78	ISIS_ste	-77.47	38.98	f090706t01p00r13	2009	7	6
79	ISIS_ste	-77.47	38.98	f090706t01p00r14	2009	7	6
80	ISIS_ste	-77.47	38.98	f090706t01p00r13	2009	7	6
81	ISIS_ste	-77.47	38.98	f090706t01p00r14	2009	7	6

Thank you!

UNIVERSITY OF MARYLAND